Heat and Mass transfer in Reactive Multilayer Systems (RMS)

M. Rühl[*1], G. Dietrich[2], E. Pflug[1], S. Braun[2] and A. Leson[2]
[1]TU-Dresden Institute of Manufacturing Technology, George-Bähr 3c, 01069 Dresden, [2] IWS Dresden, Fraunhofer Institute for Material and Beam Technology, Winterbergstraße 28, 01277 Dresden
*Corresponding author: Winterbergstraße 28, 01277 Dresden, johann.maximilian.ruehl@iws.fraunhofer.de

Abstract: Established joining techniques like welding, soldering or brazing typically are characterized by a large amount of heat load of the components. Especially in the case of heat sensitive structures like MEMS this often results in stress induced deformation and degradation or even damaging of the parts. One possible solution to avoid this problem is the use of so called Reactive Multilayer Systems (RMS). These foils consist of several hundred to a few thousand of alternating periodic reactive materials, like e. g. Al-Ni. An ignition spark activates atomic diffusion in z-direction (Figure 1) between the two reactive materials. Thus a thermal wave in x-direction (Figure 1) is generated. This wave transports the energy through the foil and activates the reaction of the materials. A self-propagation front is formed. The released heat can be used to melt solder materials (Figure 1).
A two dimensional model has been generated using COMSOL Multiphysics 3.5a. by coupling the atomic diffusion and the heat equation.

Keywords: heat transfer, atomic diffusion, multilayer, joining, Reactive Multilayer Systems

1. Introduction

Many industrial applications require the joining of heat sensitive components. Damaging of materials can be reduced by extremely short-term and localized heat input. Reactive multilayer systems (RMS) are one of the most promising candidates for such heat sources. RMS usually consist of metal components resulting in a good electrical and thermal conductivity of the joining zone.
In the 1990s Armstrong [1] and Mann et al. [2] developed the first theoretical approaches to describe the physical processes in RMS. By providing sufficient activation energy to a multilayer---for example with an electric spark or a laser pulse---an exothermal reaction of both components can be initiated. If sufficient energy is provided by the transition of the materials to their intermetalic compounds a self-propagating reaction is formed that progresses as a thermal wave through the multilayer. Theoretically the physical and chemical processes in the layers can be described as a coupled system of a two-dimensional diffusion [1-5]. This description is based on a model as shown in Figure 1. The thermal energy stimulates an atomic diffusion through the multilayer stack (z-direction). This diffusion releases enough energy that a thermal wave propagates along the layers (x-direction). The thermal wave passes through the foil with a propagation velocity v and enables atomic diffusion in neighboring areas. For this process a part of the released energy will be consumed as activation energy. The remaining energy is released as heat and can be used to melt solder layers for the joining of components. Ni/Al multilayers as described in the following are produced by magnetron sputter deposition in the Fraunhofer Institute for Material and Beam Technology, IWS [6].
In this paper we show model calculations of the physical and chemical processes in the RMS. We have calculated the propagation velocity v_{calc} and compared it with the measured velocity v_{exp}. It has also been possible to calculate the maximum temperature for several systems, e. g. by the variation of the period thicknesses from 25 to 100 nm or the atomic ratio of Al to Ni between 55 at-% to 40 at-% Al in the multilayer.

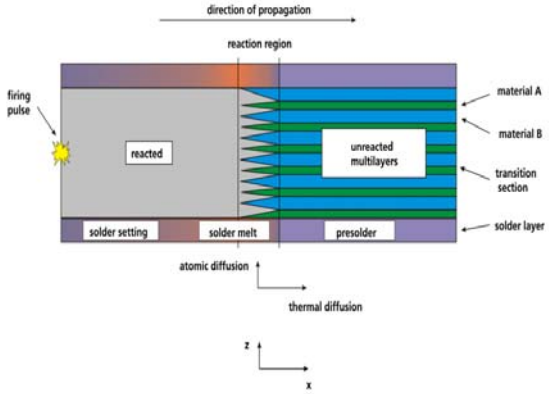

Figure 1. Principle of the atomic diffusion and the self-sustaining reaction in reactive multilayer systems.

2. Use of COMSOL Multiphysics

COMSOL Multiphysics 3.5a has been applied for the FEM simulations described in the following. In order to reduce the calculation time a two dimensional model of the RMS as a multilayer stack build with alternating layers of Al and Ni has been implemented. The period thickness of the layers is in the range from 50 nm to 100 nm. The atomic ratio N_{Al}/N_{Ni} of Al to Ni is in the range from 40 at- % to 55 at- % Al in the period. For all simulated systems 10 periods of Al and Ni layer have been calculated with a total thickness of the foil in the range between 0.5 µm and 1 µm.

In z-direction the atomic diffusion dominates the thermal diffusion by several orders of magnitude. Therefore thermal diffusion in z direction can be neglected. In the x-direction the thermal diffusion is orders of magnitude higher than atomic diffusion. Thus the model can be simplified in a way that the two differential equations have no coupling in x and z direction. Nevertheless the temperature from equation 3 couples in the atomic diffusivity (eq. 2) to activate the chemical reaction as well as in equation 1. The concentration density couples in the thermal diffusion (eq.3) by the heat source (eq. 4).

Atomic diffusion can be described by using a time-dependent scalar field $C(x,z,t)$ [mol/m³] in the diffusion equation:

$$\frac{dC(x,z,t)}{dt} - D_i \cdot \frac{\partial^2 C(x,z,t)}{\partial z^2} = 0. \qquad (1)$$

The boundary conditions in COMSOL Multiphysics used for the outside of the foil have been set to insulation/symmetry. Inside the foil it has been set to continuity. As initial values the concentrations have been set to $C_{o,Al}$ = 100 mol/m³ for Al and to $C_{o,Ni}$ = 150 mol/m³ for Ni.

For the atomic diffusivity D the Arrhenius equation has been assumed:

$$D = D_0 \cdot EXP\left(-\frac{E_A}{R \cdot T}\right). \qquad (2)$$

D_0 = $1.15 \cdot 10^{-5}$ [m/s²] is the Arrhenius preexponent of Ni and Al, E_A = 137 [kJ/mol] is the activation energy for the atomic diffusion, R [J/(mol·K)] is the gas constant and T [K] is the temperature. The atomic diffusion releases a thermal wave in x-direction. This wave can be described by the heat equation:

$$\rho_i(T) \cdot c_{p,i} \cdot \frac{\partial T(x,z,t)}{\partial t} - k_i(T) \frac{\partial^2 T(x,z,t)}{\partial x^2} = Q(C) \quad \cdot (3)$$

$c_{p,Al}$ = 897 [J/(kg·K)], $c_{p,Ni}$ = 444 [J/(kg·K)] are the heat capacities, $\rho_i(T) = \rho_{0,i}/(1+3 \cdot \alpha_i \cdot (T-T_0))$ [kg/m³] is the temperature dependent density, with $\rho_{0,Al}$ = 2700 [kg/m³], $\rho_{0,Ni}$ = 8908 [kg/m³], α_{Al} = $23.1 \cdot 10^{-6}$ [1/K] and α_{Ni} = $13.4 \cdot 10^{-6}$ [1/K] is the thermal expansion coefficient. The thermal conductivity $k_i(T) = (L \cdot T)/(R_{s,0,i} \cdot (1+\alpha \cdot (T-T_0)))$ [W/(m·K)], L = $2.45 \cdot 10^{-8}$ [V²/K²] the Lorenz number and $R_{s,0,Al}$ = $2.65 \cdot 10^{-8}$ [Ω·m] and $R_{s,0,Ni}$ = $6.93 \cdot 10^{-8}$ [Ω·m] the specific electrical resistance.

For the concentration dependent heat source $Q(C)$ [W/m³] an ansatz from [1] is used:

$$Q = \frac{H \cdot M^2}{\rho(T)} \cdot \left(\frac{\partial C(x,z,t)^2}{\partial t} + v_{Diff} \cdot \frac{\partial C(x,z,t)^2}{\partial x} \right) \qquad (4)$$

H [kJ/g] is the enthalpy of the reactive foil, which was measured with differential thermo analysis (DTA) and has values between H = 1 – 2.1 [kJ/g] in dependence of the Al to Ni atomic ratio. M [kg/mol] is the molar mass of the reactants and v_{Diff} [m/s] is the diffusion velocity.

To simulate the activation of the atomic diffusion, an ignition spark ZF (eq. 5) with a Gauss profile has been used:

$$ZF = T_0 + T_I \cdot EXP\left(-\frac{t^2}{2 \cdot t_i}\right). \qquad (5)$$

T_0 = 293 [K] is the room temperature, T_I = 2000 [K] is the spark temperature, t_i = $5 \cdot 10^{-10}$ [s²] is the ignition time. ZF has been used as boundary condition temperature at x = 0 to activate the reaction. In the opposite direction the boundary condition temperature has been set to T_0, the sides of the foil have been set to "convective flux". Inside the foil "continuity" has been used as boundary condition. The solver PARADISO has been used for the time dependent calculation with a solution time from 0 to 600 µs and an output time of 10 µs. An individual mesh for each Al- and Ni-layer has been introduced taking into account the period thickness d_p and the Al to Ni atomic ratio.

3. Propagation velocity v

The propagation velocity *v* of the RMS has been measured to verify the model. Ignition was provided by a short and localized electric pulse. The propagation velocity *v* of the thermal wave has been measured with a high-speed camera mounted on a tripod. The propagation velocity *v* (Figure 2) is equal to the distance *s* the thermal wave moved within a certain number of images *n* and the time between two frames Δt:

$$v = \frac{s}{n \cdot \Delta t} . \qquad (6)$$

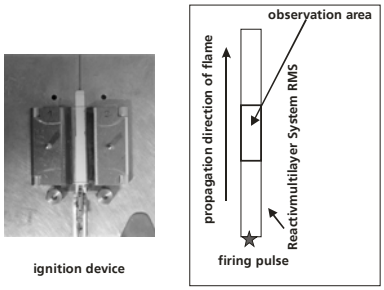

Figure 2: Ignition device for measuring the propagation velocity *v*.

The results of the simulation have been compared with the measured propagation velocity v_{exp}.

4. Results and discussion

In the following the results for the temperature *T(x,z,t)* and the propagation velocity v_{calc} are presented and compared to the measured velocity v_{exp}.
Figure 3 shows the temperature distribution *T(x,z,t)* of a RMS, with a length L = 0.6 mm, a total thickness d_{tot} = 0.5 µm and a period thickness d_p = 50 nm:

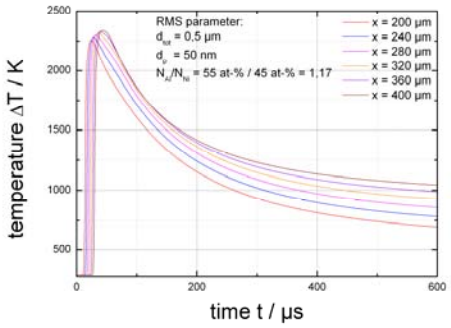

Figure 3: Temperature T(x,z,t) distribution as a function of the time and the propagation position x of the thermal wave.

A maximum temperature *T(x,z,t)* of 2340 K has been calculated, a propagation velocity v_{calc} of 9.7 m/s and a melting time for a tin-solder of $t_{m,Sn} > 1$ ms.

In Figure 4 the corresponding concentration *C(x,z,t)* is shown. It turns out that Ni and Al interact with each other. In the end of the reaction the intermetallic phase NiAl is formed. The model corresponds to X-ray diffraction experiments; that intermetallic phase is the final state of the reaction in the RMS.

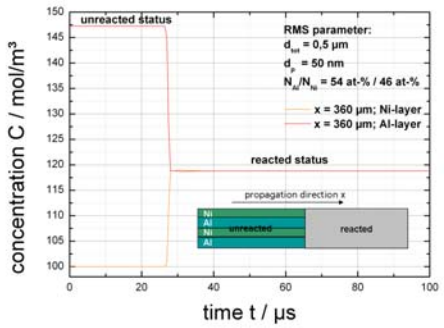

Figure 4: Concentration *C(x,z,t)* as a function of time and propagation position x of the thermal wave.

Figure 5 illustrates the temperature *T(x,z,t)* as a function of the period thickness d_p. For a smaller periodic thickness the propagation velocity is higher and therefore the temperature peak width is smaller and the maximum temperature is higher (Figure 6). Figure 5 shows increasing maximum temperatures with decreasing period thicknesses.

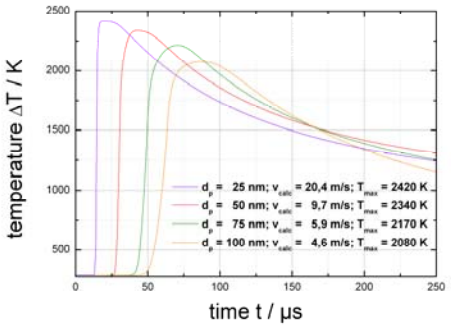

Figure 5: Temperature field *T(x,z,t)* as a function of the period thickness d_p.

In Figure 6 the calculated propagation velocity v_{calc} is compared with the velocity v_{exp} obtained from experiments. The calculated velocity v_{calc} is about 30 % higher than the v_{exp}. The reason for this behaviour is the assumption of an ideal model without any impurity of the material and inter-diffusion zones between the layers in the calculation for v_{calc}. This model has to be adapted to the experimental results.
With increasing the period thickness d_p the diffusion lengths are also increased. It is expected that this results in a decreasing v_{calc} . For the experimental results the same exponential fit-function can be used as for the calculations. This is an indication for the quality of the model.

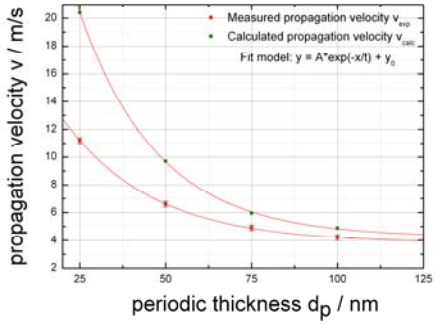

Figure 6: Comparison of the measured velocity v_{exp} and the calculated velocity v_{calc} as function of the period thickness d_p.

Figure 7 shows the different temperatures *T(x,z,t)* for different Al to Ni atomic ratios. The parameters of the RMS were d_{tot} = 0.5 µm, d_p = 50 nm and L = 0.8 mm only the atomic-ratio has been modified.

An atomic-ratio of N_{Al}/N_{Ni} = 50 at-%/50 at-% produces the highest values for temperature and v_{calc}, because of the highest energy content. Deviations from this ratio result in lower temperatures and velocities. The maximum temperature and propagation velocity *v* decrease with an increasing amount of Al or Ni in the period.

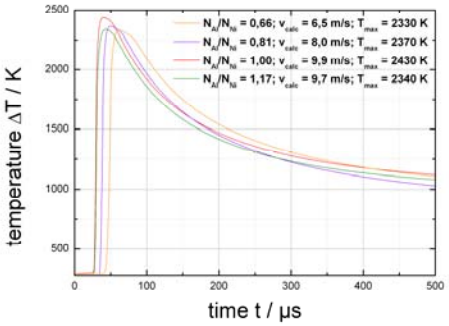

Figure 7: Temperature field *T(x,z,t)* as a function of the time and the Al to Ni atomic ratio.

In figure 8 the calculated and experimentally measured propagation velocities *v* are compared as a function of the Al to Ni ratio in the range of 40 at-% to 55 at-% Al. Again, the calculated velocity v_{calc} is higher then the measured one. The reason is the same as above: the assumption of ideal layers without any impurities and inter-diffusion zones results in the overestimation of the velocity. It can be seen that, if the Ni content in the period is increased, in agreement with the measurements the velocity is lower.

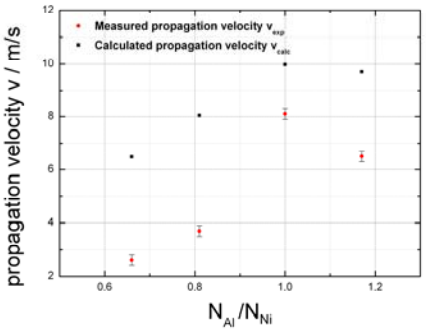

Figure 8: Comparison of the measured velocity v_{exp} and the calculated velocity v_{calc} as function of the Al to Ni atomic ratio.

5. Conclusions

With the atomic heat transfer models the chemical and physical processes in reactive multilayer systems have been described. The model has been verified by the comparison of the maximum temperatures and the velocities v_{exp} and v_{calc} of the reaction front. The maximum temperature could be confirmed.
Joining applications need the right temperature to the right time in order to melt the solder between the components. Available parameters for changing temperature, propagation velocity and melting time are the period thickness d_p, the atomic ratio Al to Ni and the total thickness. Based on the calculations tailored multilayer designs can be fabricated for specific applications. This opens the perspective for the utilization of reactive multilayer systems in a broad range of industrial applications.

6. References

1. R. Armstrong, Theoretical models for the combustion of alloyable materials, *Metallurgical and Materials Transactions A*, **Vol.23**, 2339 No.9 (1992)
2. A.B. Mann, A.J. Gavens, M.E. Reiss, D. Van Heerden, G. Bao, T.P. Wheis, Modeling and characterizing the propagation velocity of exothermic reactions in multilayer foils, J. Appl. Phys., **Vol.82**, 1178 (1997)
3. S. Jayaraman, O.M. Knio, A.B. Mann, T.P. Weihs, Numerical predictions of oscillatorycombustion in reactive multilayers, *J. Appl. Phys.* , **Vol.86**, 800 (1999)
4. M. Salloum, O.M. Knio, Simulation of reactive nonolaminates using reduced models: I. Basic formulation. , *Combustion and Flame*, **Vol.157**, 288-295 (2010)
5. M. Salloum, O.M. Knio, Simulation of reactive nonolaminates using reduced models: II. Normal propagation. , *Combustion and Flame*, **Vol.157**, 436-445 (2010)
6. G. Dietrich, M. Rühl, S. Braun, A. Leson, Hochpräzise Fügungen mittels reaktiven Nanometermultischichten, *Vakuum in Forschung und Praxis*, **Vol.24**, 9 No.1 (2012)